DOI 10.1007/s11094-024-03056-7
Pharmaceutical Chemistry Journal, Vol. 57, No. 10, January, 2024 (Russian Original Vol. 57, No. 10, October, 2023)

SYNTHESIS, ANTIMICROBIAL, AND DNA-BINDING EVALUATION OF NOVEL SCHIFF BASES CONTAINING TETRAZOLE MOIETY AND THEIR NI(II) AND PT(II) COMPLEXES

M. Ulular,[1] N. Sarı,[1,*] F. Han,[1] H. Öğütcü,[2] and E. Hasanoğlu Özkan[1]

Original article submitted October 9, 2022.

Ni(II) and Pt(II) complexes of tetrazole-containing Schiff bases were synthesized and characterized by physicochemical and various spectroscopic studies. To examine its potential as a candidate anticancer drug, the binding properties of ct-DNA were investigated. The characteristic binding constant (K_b) and binding mode of the complexes with calf thymus DNA (ct-DNA) were determined using absorption titration (1.99 – 76.71 × 10^4 M^{-1}). According to the kinetic and thermodynamic parameters, the binding constant and spontaneity of the Pt(Tet-SalH) complex were found to be larger. The well-diffusion method was used to deduce the antibacterial potency of Schiff bases and their complexes. All these substances have been examined for antibacterial activity against pathogenic strains and antifungal activity. Only complex [Pt(3,5-Br-Sal-Tet)H_2O]Cl·H_2O showed activity against all the microorganisms studied.

Keywords: Schiff bases; tetrazole; Pt(II) complexes; calf thymus DNA; antimicrobial activity; pathogen microorganisms.

1. INTRODUCTION

The ability of base pairs or phosphate groups contained in DNA to bind selectively to organic and inorganic species has led to increased synthesis of potential chemotherapy agents. Schiff bases with different properties have antifungal, analgesic, anti-inflammatory, antibacterial, antioxidant, antitumor, and antituberculosis effects [1]. Cu(II) and Gd(II) complexes of Schiff bases are known to be used in MR imaging [2]. The presence of a donor atom in the structure of Schiff bases has led to increased studies on complex formation reactions. Schiff bases forming the coordination compound may give one or more electron pairs to the metal ion [3, 4]. In addition, the corrosion inhibitory properties of Schiff bases provide another area of use [5].

Heterocyclic compounds are used in the treatment of many diseases (including cancer). Biological molecules such as DNA, RNA, vitamins in metabolism contain heterocyclic rings in their structure, which has led to the importance of heterocyclic compounds in the medical field. Compounds such as indoles, benzothiazole, camptothecin, benzimidazole, and benzothiazole, which have a heterocyclic ring in their structure, are in the category of anticancer drugs. Likewise, tetrazole-containing heterocyclic rings have been involved in numerous studies in recent years because tetrazole and its derivatives have antihypertensive, antifungal, antituberculosis, antimalarial, antidiabetic, and anticancer properties [6].

Tetrazoles are heterocyclic compounds formed by one carbon atom and four nitrogen atoms and contain two unsaturations [7]. Tetrazole is a condensation product of Zionegen and phenylhydrazine discovered by Bladin in 1885. It was found during the study of dicyanophenylhydrazine [8]. The tetrazole ring has a stable structure. The π electron system in the tetrazole ring and the presence of an electron pair on the N atom cause it to interact with various electrophilic substances [9].

The tetrazole molecule is planar and is an aromatic compound with a total of six electrons [10]. The pH of the tetrazole molecule is close to the pH of the carboxylic acid molecule (pK_a 4.76). Tetrazoles, which are more stable than carboxylic acid groups, are preferred in newly developed drugs.

One of the promising compounds, the diversification of tetrazoles is important for medicinal chemistry because it has a wide range of different biological activities, such as antifungal and antibacterial. It can also mimic enzymatic reac-

[1] Department of Chemistry, Faculty of Science, Gazi University, 06500 Teknikokullar, Ankara, Turkiye.
[2] Department of Field Corps, Faculty of Agriculture, Kırşehir Ahi Evran University, Kırşehir, Türkiye.
[*] e-mail: nursens@gazi.edu.tr

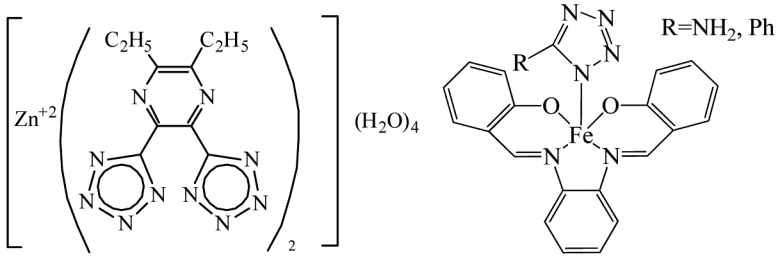

Fig. 1. Dinuclear Zn(II) complex and Fe(II) complex with a five-coordination.

tions owing to its similarity to carboxylic acid functions. Therefore, tetrazoles have broad biological and pharmacological properties. Currently, tetrazole-based drugs such as cefamandole, ceftezole, losartan, iosartan, valsartan, cefazolin, and cefoperazone are used clinically. However, the widespread distribution of drug-resistant bacteria and emerging new pathogenic organisms has created a need for the development of new antibacterial agents.

Moreover, *N*-unsubstituted tetrazoles have been widely used in the pharmaceutical industry in recent years [11]. Tetrazole is often used in medicinal chemistry, the explosives industry and materials science. The anticancer mechanisms of tetrazole-based drugs are explained on the basis of PRMT, COX-2, tubulin polymerization, efflux pump, and HIF-1α [12].

The reaction of tetrazoles with metal ions and salts has been known for half a century. One of the most important areas in which coordination complexes containing tetrazole are used is in medicinal chemistry. Owing to the high physiological activity and low toxicity of complexes containing tetrazole, its use in areas such as biochemical and pharmaceuticals is valuable. For example, Cu(II), Co(II), Ni(II), and Zn(II) complexes of the cefazolin derivative used as an antibiotic show higher activity in vitro than some bacterial strains. In addition, tetrazoles are used as components of a new generation of filter materials for the purification of biological fluids (blood, lymph, etc.) from heavy metal ions [13]. Metal atoms are bonded to the heterocyclic molecule by covalent, ionic, or coordinated covalent bonding and as a result of this bonding, the structure is neutral, anionic or cationic [14]. Tetrazole-containing coordination compounds can be found in one-, two- or three-nuclear structures [15]. In Figure 1, the complexes with a four- or five-coordination structure can be given as an example [16].

Elucidating the antitumor properties of complexes requires a better understanding of the binding between the complex and DNA. Thus, it may guide the design of new types of antitumor drugs. This research was aimed at developing alternative structures based on different metals instead of platinum(II), which may have therapeutic and better pharmacological properties. In this work, we decided to design the first Schiff base-containing tetrazoles with the idea that modification of the tetrazole compound may improve antibacterial and antimalarial properties.

Furthermore, the electronic configuration and oxidation state of metal ions and the geometry of metal complexes are known to exert different effects on biological molecules and

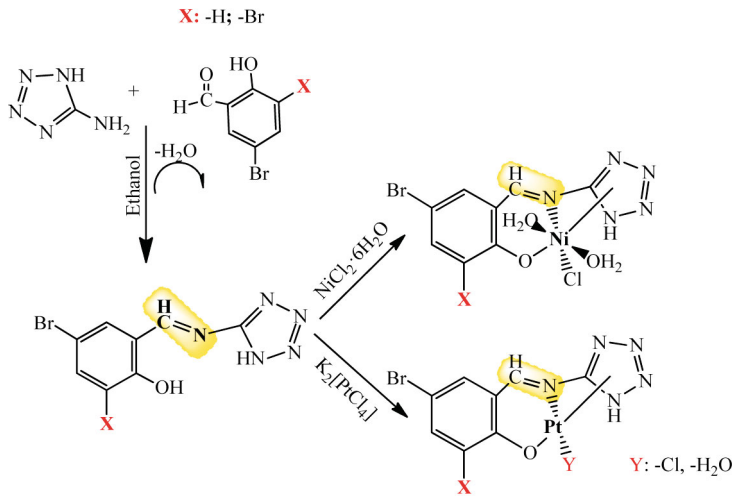

Fig. 2. General procedure for the synthesis of Schiff bases and their Ni(II) and Pt(II) complexes.

planar molecules show strong antitumor activity because they have better DNA binding properties.

As Pt(II) complexes are usually planar, the Pt(II) ion was chosen in this study. The Ni(II) ion has the same configuration (d^8) as the Pt(II) ion and was chosen to compare its antimicrobial and DNA binding properties with the Pt(II) ion.

Therefore, first, 5-aminotetrazole and 5-bromosalisilaldehyde and 3,5-dibromosalisilaldehyde (5-Br-Sal-Tet) and (3,5-Br-Sal-Tet) coded Schiff bases were synthesized by means of a condensation reaction (Fig. 2). The structures of the Schiff bases were elucidated by FT-IR, ^{1}H-NMR, ^{13}C-NMR, UV-GB spectra, and elemental analyses. Then Ni(II) and Pt(II) complexes of Schiff bases were synthesized according to the template method and their structures were elucidated by spectral and thermal analysis, magnetic susceptibility measurements, and elemental analysis. A DNA binding study was carried out using electronic absorption spectroscopy of all synthesized compounds and DNA binding constants were determined using the Vant Hoff equation. Furthermore, viscosity measurements were performed by keeping the calf thymus (ct)-DNA concentration constant and varying the concentration of tetrazolato ligands and their complexes.

2. EXPERIMENTAL

2.1. Materials and Methods

The materials were all of reagent grade (Sigma-Aldrich Company). A Thermo Scientific Flash 2000 organic elemental analyzer device was used for the elemental studies. NMR spectra of the studied Schiff bases and Pt(II) complexes were recorded with a Bruker Spectrospin Avance DPX-400 instrument using TMS as an internal standard and DMSO-d_6 as a solvent. IR spectra were recorded ranging from 4000 to 450 cm^{-1} on a Mattson-1000 FT-IR instrument. Thermal gravimetric analysis (TGA) of the Ni(II) and Pt(II) complexes was recorded by a Setaram simultaneous model thermal analyzer under nitrogen atmosphere between 20°C and 900°C at a heating rate of 10°C min^{-1}. Conductivity measurements were carried out at 23 ± 0.1°C in 10^{-3} M DMSO using an inoLab Cond 730 apparatus. The room temperature magnetic moments were measured using an MK-1 model Gouy Balance of Christison Scientific Equipment Ltd. Metal contents were determined by using a Philips PU 9285 atomic absorption instrument. Spectroscopic DNA binding studies were performed using a UV-Visible spectrophotometer (Shimadzu-1800, ENG240V) within the range 1100 – 1200 nm.

2.2. Synthesis of Schiff Bases and Their Complexes

General Synthesis of Schiff Base Including Tetrazole; (5-Br-Sal-Tet) and (3,5-Br-Sal-Tet)

A mixture of aldehyde 2.5×10^{-3} mol (5-bromosalicylaldehyde, 3,5-bromosalicylaldehyde) in EtOH (20 mL) was added dropwise to the 25 mL hot EtOH solution of the 5-aminotetrazol (2.5×10^{-3} mol) and heated under reflux for 3 h. After cooling, the mixture was filtered and allowed to stand. After this time, the mixture remaining in the beaker was kept for 4 days and solid product was filtered through filter paper and dried in an oven at 70°C for 3 h.

General Synthesis of Complexes; ([Ni(5-Br-Sal-Tet)], [Ni(3,5-Br-Sal-Tet)], [Pt(5-Br-Sal-Tet)], [Pt(3,5-Br-Sal-Tet)])

Ni(II) and Pt(II) complexes of Schiff base ligands resulting from the condensation of 2.5×10^{-3} mol of aldehyde with 2.5×10^{-3} mol of 5-aminotetrazol has been isolated by metal template reaction. A sample of $NiCl_2 \cdot 6H_2O$ and $K_2[PtCl_4]$ was dissolved in 15 mL ethanol. To this solution, 5-aminotetrazol (2.5×10^{-3} mol) and aldehyde (5-bromosalicylaldehyde, 3,5-bromosalicylaldehyde; 2.5×10^{-3} mol) in 10 mL ethanol were added, giving a colored solution. The resulting solution was stirred for approximately 2 h under reflux, filtered, and allowed to stand. On standing for a further 5 days (10 days for Pt(II) complexes), the solid complexes formed were collected by filtration, washed with ethanol:acetone (1:1), and then filtered through filter paper and dried in an oven at 80°C.

2.3. Studies on DNA Binding and Antimicrobial Activity

Research on Viscosity

Viscosity measurements were performed by keeping the ct-DNA concentration constant (0.5 μM) and varying the concentration of the Schiff bases ligand and their complexes. 35-μM solutions were prepared in Tris-HCl/NaCl buffer of Schiff bases ligand and their complexes. Utilizing an Ubbelohde Viscometer at 37°C, viscosity studies were conducted [17]. The data were presented as $(\eta/\eta_o)^{1/3}$ versus [compound]/[DNA] ratio (η_o and η are the viscosity of DNA in the absence and presence of compounds respectively). (η_o: the viscosity of DNA in the absence of compounds, η: the viscosity of DNA in the presence of compounds).

UV Absorption Studies

The solid form of ct-DNA was purchased from Sigma-Aldrich and dissolved at room temperature using a buffer solution of 5 mM Tris-HCl/50 mM NaCl (pH 7.2). It was prepared daily and stored at +4°C. The molar concentration of ct-DNA was determined using both the absorbance value measured at a wavelength of 260 nm and molar absorption coefficient ($\varepsilon = 6600\ M^{-1}cm^{-1}$) [18]. All synthesized

molecules were dissolved in DMSO to prepare the stock solution. The 85-μM concentration that was used in the study was prepared using the stock solution. For the study of DNA interactions, solutions of compounds (ligands and complexes) with a concentration of 85 μM were prepared from stock solutions. While investigating the interactions of ligands and complexes with CT-DNA, a concentration of 85 μM was kept and increasing amounts of CT-DNA solution of known concentration ($1.3^{-1}0^{-3}$ M) were added; thus, a series of (compound) + CT-DNA solutions (0.2 mL; 0.4 mL; 0.6 mL; 0.8 mL; 1.0 mL) were prepared. To prepare these solutions, the total volume (2 mL) was completed with Tris-HCl/NaCl buffer (5-min incubation at room temperature), its absorbance within the wavelength range 200 – 500 nm was measured using UV-Vis spectrophotometry.

The DNA concentration ([DNA]) against $[DNA]/(\varepsilon_a–e_f)$ plots were drawn using the results. The slope of the plot was calculated as $1/(\varepsilon_b–e_f)$, its intersection was calculated as $1/K_b(\varepsilon_b–e_f)$, and the attachment coefficients (K_b) were calculated by proportioning the two values (Eq. 1):

$$[DNA]/(\varepsilon_a\text{-}e_f) = [DNA]/(\varepsilon_b–e_f) + 1/K_b(\varepsilon_b–e_f) \quad (1)$$

The change in absorbance intensity was given in percentages using (Eq. 2) and the standard free energy, DG°, value was calculated (Eq. 3).

$$H\% = [(A_i\text{-}A_s)/(A_i)]^{-1}00\% \quad (2)$$

$$DG° = –R.T.\ln K_b \quad (3)$$

(H%: The percentage change in absorbance intensity (hypochromism or hyperchromism; Ai: absorbance intensity of the free compound before the addition of DNA; As: absorbance intensity of the compound after the addition of DNA at maximum concentration)

Detection of Antimicrobial Activity

The Schiff bases and their Ni(II) / Pt(II) complexes were tested for their antimicrobial activity by the well-diffusion method [19, 20]. Each Schiff base and complex was kept dry at room temperature and dissolved (0.018 μg/mL) in DMF. DMF was used as a solvent and also for control. It was found to have no antimicrobial activity against any of the tested organisms. 1% (v/v) of 24-h broth culture containing 10^6 CFU/mL was placed in sterile Petri dishes. The study was continued in accordance with the literature [21].

3. RESULTS AND DISCUSSION

3.1. Characterization Studies of Schiff Bases and Their Complexes

Elemental Analysis and Spectra of Schiff Bases Including Tetrazole

The complexes and ligands were soluble in polar organic solvents but not in apolar solvents. As seen in Tables 1 and 2, the elemental analysis results are in agreement with the proposed structures. IR bands of (5-Br-Sal-Tet) and (3,5-Br-Sal-Tet), in the 1652 cm^{-1} and 16277 cm^{-1}, 3471 and 3435 cm^{-1}, 3373 cm^{-1}, and 3372 cm^{-1} regions are characteristic of n(CH=N), n(OH), and n(NH) respectively [22]. The n(N=N) stretching frequencies were observed within the range 1501 cm^{-1} to 1523 cm^{-1} and the n(C-Br) vibrations were observed at 630 cm^{-1} [23]. In UV spectra of (5-Br-Sal-Tet) and (3,5-Br-Sal-Tet), intense multiple bands emerged between 200 nm and 245 nm in the UV region.

These bands were attributed to the $\sigma \rightarrow \sigma^*$ and $n \rightarrow \sigma^*$ transition of the aromatic ring. The moderately intense bands within the range 310 nm to 330 nm were attributed to the $\pi \rightarrow \pi^*$ transition due to the imine group.

When the NMR spectra of the ligands were analyzed in detail, the chemical shift value of –NH in the tetrazole ring of the ligands is consistent with the literature. It has been reported that the chemical shift value of –NH in the aromatic ring tetrazole compound containing an oxide group can be between 13.50 and 15.50 ppm [24, 25] (Figure 3). The chemical shifts at 8.00 and 9.80 ppm for (5-Br-Sal-Tet) and (3,5-Br-Sal-Tet) ligands and 9.49/9.80 and 9.50/10.30 ppm

TABLE 1. Analytical Data, Some of the Physical Properties, IR, and UV Spectra Data of Ligands

Symbol Formula, (M_w, g·mol^{-1})	Conductivity in solvent (*), color/m.p. (°C)	Elemental Analysis Found (Calculated)%			$\nu_{NH(arom)}/\nu_{N=N}$ $\nu_{–OH}/\nu_{–CH=N}$ //$\nu_{C–Br}$	λ_{max} (Abs, nm)
		C	H	N		
(5-Br-Sal-Tet) $C_8H_9BrN_5O_3$ (302.98)	17.4 yellow/165	32.0 ± 0.01 (31.68)	3.07 ± 0.02 (2.97)	22.20 ± 0.02 (23.10)	3373,776/1501 3471/1652/627	200–245 (3.40 – 3.70 m), 275 (0.48), 310 (0.01)
(3,5-Br-Sal-Tet) $C_8H_5Br_2N_5O$ (346.88)	27.3 light yellow/153	27.40 ± 0.02 (27.69)	1.46 ± 0.02 (1.45)	21.01 ± 0.03 (20.18)	3332,769/1523 3335/1627//630	200–240 (3.76–3.20 m), 250 (0.47), 330 (0.2)

* (Ω^{-1} cm^2 mol^2)

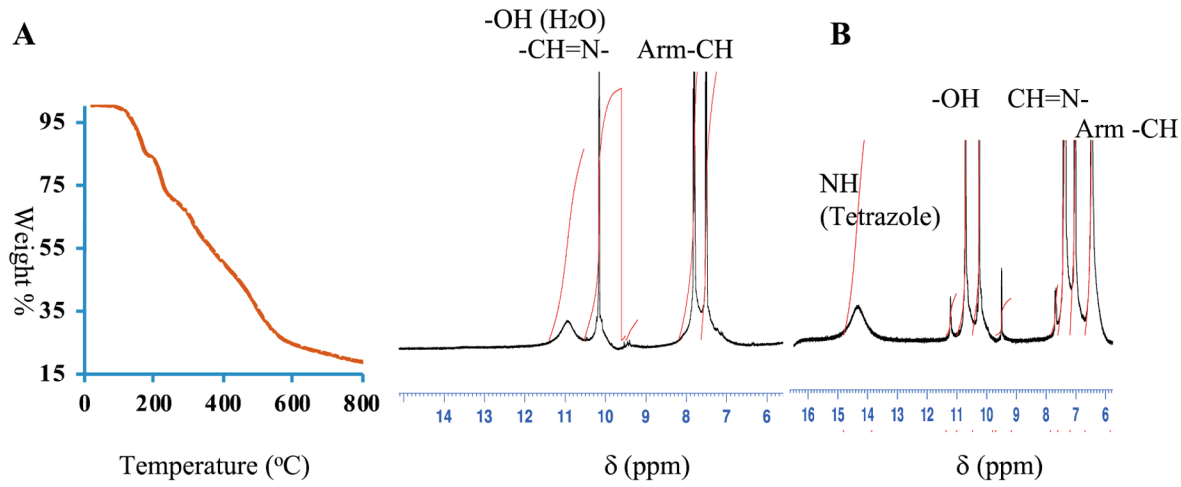

Fig. 3. **A**: TGA and ^{1}H-NMR for [Pt(3, 5-Br-Sal-Tet)H_2O]Cl. H_2O; **B**: ^{1}H-NMR for (3,5-Br-Sal-Tet).

due to the tautomeric structure were suggested to correspond to –CH=N and =CH-NH /=CH-NH respectively.

As is known, the α-H-containing carbonyl and imine compounds can show keto-enol tautomerism. The keto-enol tautomerism was detected in two of the prepared Schiff bases according to their NMR spectra. In the Schiff bases coded (5-Br-Sal-Tet) and (3,5-Br-Sal-Tet), the peak at 11.18 ppm and 12.71 ppm is thought to refer to the proton in the –OH group.

The appearance of the characteristic multiple peaks belonging to the aromatic ring within the range 7.01–8.18 ppm was considered as evidence that the aldehyde was incorporated into the tetrazole compound. ^{13}C peaks of ligands are given in Table 2.

Elemental Analysis and Spectra of Complexes

Elemental analyses are compatible with the proposed structures, and their conductivity in DMF (10^{-3}M) medium was found to be within the range 8.7 – 113.4 Ω^{-1} cm^2 mol^2 (Table 3). The results showed that all complexes were conductive in the 1:1 type except [Pt(3,5-Br-Sal-Tet)H_2O]Cl · H_2O [3, 4]. The effective magnetic moments of the complexes were calculated and it was found that the Ni(II) complexes are paramagnetic, the magnetic moments were calcu-

TABLE 2. ^{1}H and ^{12}C NMR of Schiff Bases Including Tetrazole

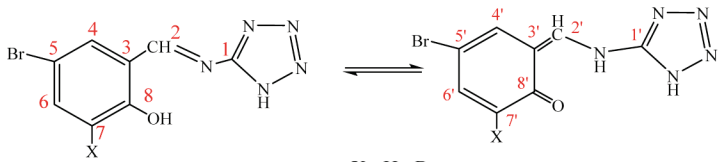

Symbol	^{1}H-NMR data (ppm)			^{13}C-NMR data (ppm)		
	=CH-NH(keto)/$NH_{(Tet)keto}$/–OH/–$NH_{(Tet)enol}$	–CH=N/ CH(arom)	C_1, C_1	C_3, C_3	C_5, C_5	C_7, C_7
			C_2, C_2	C_4, C_4	C_6, C_6	C_8, C_8
(5-Br-Sal-Tet)	9.82 (s)/6.46/11.18 (s)/n.o	9.49 (s)/7.67–7.01 (m)	165.96 157.39	120.80 n.o.	156.80 157.41	119.60 112.78
			156.61 157.18	114.80 95.06	121.06 153.20	154.30 190.01
(3,5-Br-Sal-Tet)	10.30 (s)/6.47/12.71 (s)/14.25	9.50(s)/8.18–7.28 (m)	168.02 n.o.	121.63 124.50	113.40 112.50	111.70 111.36
			156.85 156.39	135.01 133.67	140.99 139.88	157.80 193.67

s: single, m: multiple, n.o.: not observed

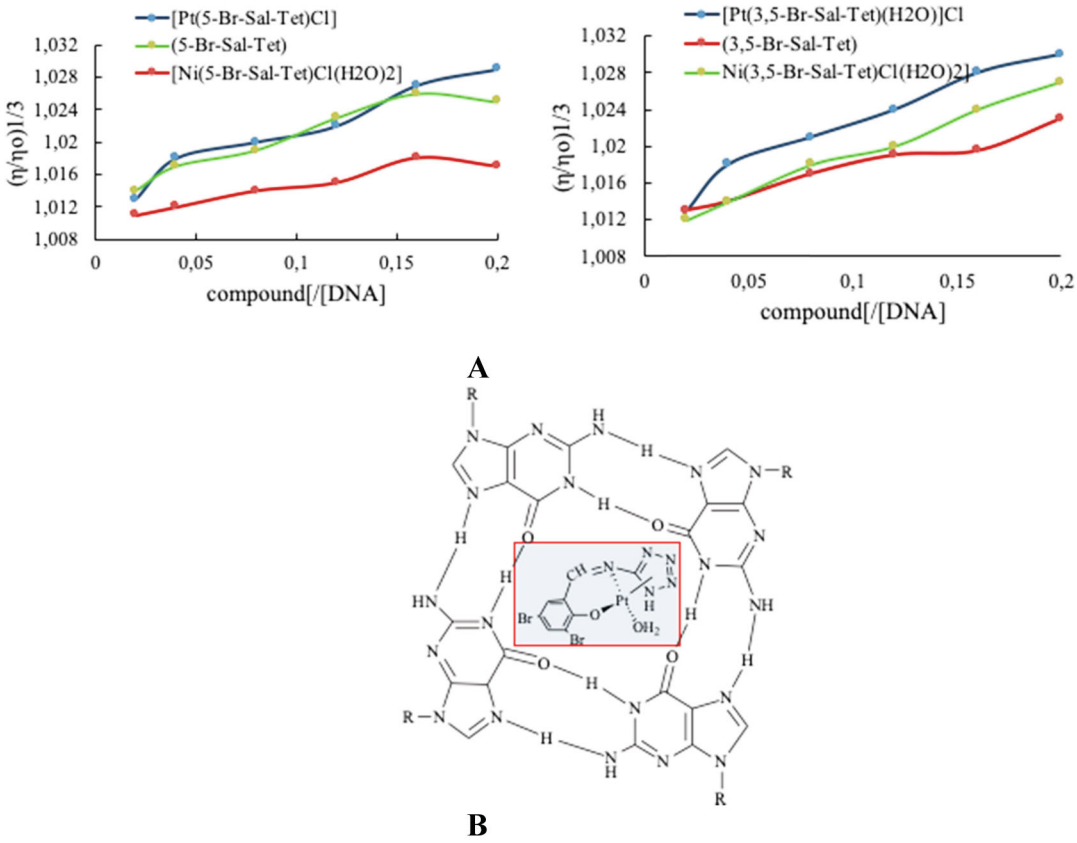

Fig. 4. A: Plot of relative specific viscosity of Schiff bases and their complexes against [compound]/[DNA] at physiological temperature (37°C). **B:** Schematic representation of the possible P–P interaction between G-quadruplexes and the Pt(II) complex.

lated as 3.88 and 4.07 BM for $[Ni(5\text{-Br-Sal-Tet})Cl(H_2O)_2] \cdot 2H_2O$ and $[Ni(3,5\text{-Br-Sal-Tet})Cl(H_2O)_2] \cdot 2H_2O$ respectively. These values correspond to two unpaired electrons. Pt(II) complexes were found to be diamagnetic. One of the bands corresponding to the d-d transitions of Ni(II) complexes (1×10^{-3}M) was observed. This band belongs to the

TABLE 3. Analytical Data, Some of the Physical Properties, and TGA Analysis of Schiff Bases Complexes

Symbol Mw (g/mol)	Conductivity (*), m.p. (°C)/color, $\mu_{eff\,(B.M.)}$	Elemental Analysis Found (Calculated)%			Thermal Analysis		
		C	H	N	% $^{a}H_2O$ t (°C)	% $^{b}H_2O$ t (°C)	% r.m. t (°C)
$[Ni(5\text{-Br-Sal-Tet})Cl(H_2O)_2] \cdot 2H_2O$ 433.27	8.7, 130 – 132/turquoise, 3.88	22.50 ± 0.04 (22.18)	2.18 ± 0.01 (3.02)	16.40 ± 0.02 (16.16)	7.40 (116)	8.20 (150)	r.l.m. 150 – 800
$[Pt(5\text{-Br-Sal-Tet})Cl] \cdot H_2O$ 533.62	32.7, 116 – 121/light red, D	17.01 ± 0.01 (16.88)	1.67 ± 0.03 (1.59)	12.12 ± 0.04 (12.31)	1.08 (120)	5.04 (190)	21.7 190 – 800
$[Ni(3,5\text{-Br-Sal-Tet})Cl(H_2O)_2] \cdot 2H_2O$ 512.18	12.9, 93 – 95/turquoise, 4.07	18.81 ± 0.04 (19.44)	1.62 ± 0.02 (2.04)	14.14 ± 0.02 (14.17)	8.9 (117)	6.8 (179)	21.7 180 – 800
$[Pt(3,5\text{-Br-Sal-Tet})H_2O]Cl \cdot H_2O$ 612.52	113.4, 85 – 88/orange, D	15.02 ± 0.02 (15.24) ± 0.03	1.57 ± 0.04 (1.60) ± 0.02	11.90 ± 0.03 (11.11) ± 0.04	1.58 (115)	4.7 (185)	21.3 185 – 800

(*): Ω^{-1} cm^2 mol^2, D: diamagnetic; r.m.: remaining mass; r.l.m.: rapid loss of mass;
[a]: crystal water; [b]: coordination water

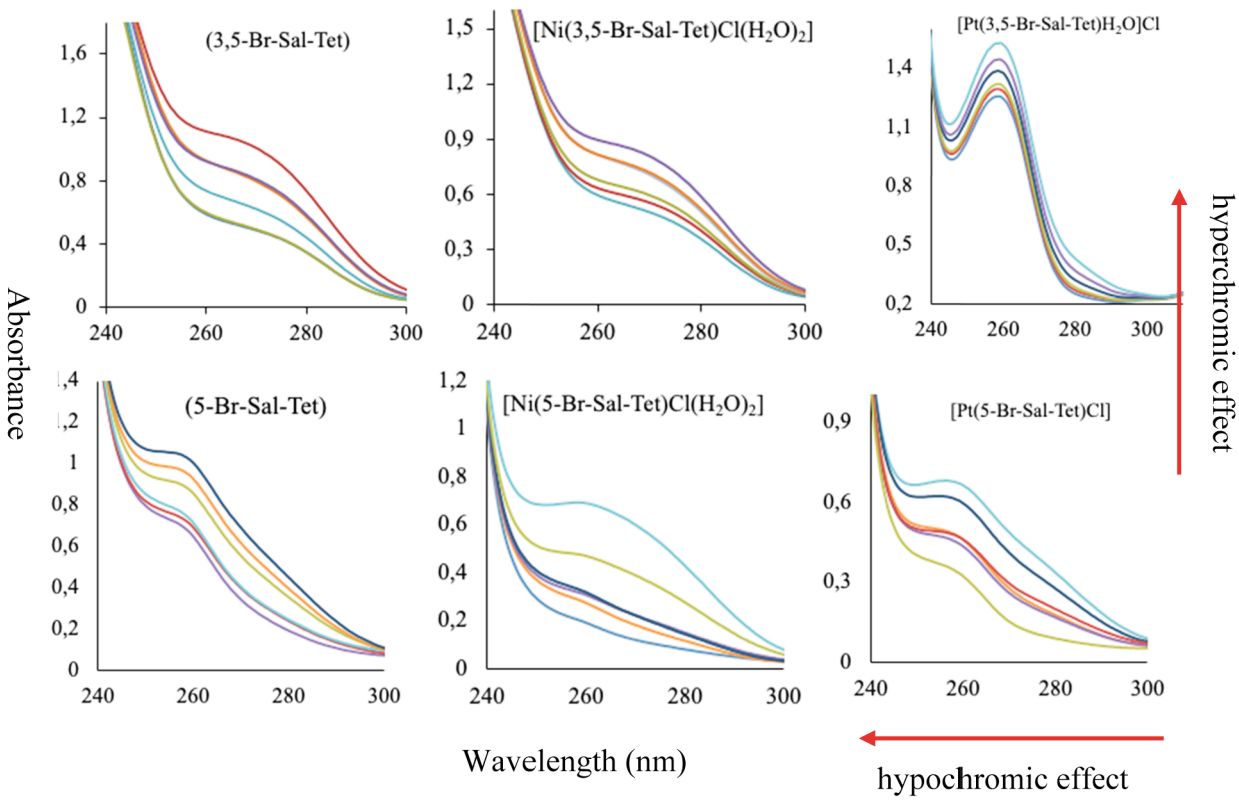

Fig. 5. UV-visible spectra of ligands and their Ni(II), Pt(II) complexes in the presence of ct-DNA. Arrow direction indicates the trend in absorption in the presence of increasing DNA concentrations.

$A_{2g} \rightarrow T_{1g}$ transition and was observed at a wavelength of 369 nm and 380 nm for $[Ni(5\text{-Br-Sal-Tet})Cl(H_2O)_2] \cdot 2H_2O$ and $[Ni(3,5\text{-Br-Sal-Tet})Cl(H_2O)_2] \cdot 2H_2O$ respectively.

The thermal properties of $[Ni(3,5\text{-Br-Sal-Tet})Cl(H_2O)_2] \cdot 2H_2O$ and $[Pt(3,5\text{-Br-Sal-Tet})H_2O]Cl \cdot H_2O$ were examined using TGA and important results are given in Table 3.

The mass losses around 100°C observed in the TGA curves were thought to be due to crystal water and mass losses above 130°C were thought to be due to coordination water. As seen from the curve, the mass loss of the $[Ni(3,5\text{-Br-Sal-Tet})Cl(H_2O)_2] \cdot 2H_2O$ complex was suggested to be equivalent to a mass loss due to 117°C crystal water in TGA analysis, which was determined to correspond to 1 mole of water. The coordination water at 149.16°C was thought to correspond to 2 moles of water. As seen in the TGA curve of the $[Pt(3,5\text{-Br-Sal-Tet})H_2O]Cl \cdot H_2O$ complex, the mass loss was determined to be due to the crystal water at 115°C and corresponded to 1 mole of water. The coordination water was thought to correspond to 1 mole of water at 135°C.

The characteristic peaks of the FT-IR spectra of Ni(II) and Pt(II) complexes are given in Table 3. In all complexes, –OH stretching vibrations of crystalline water, aromatic –C–H vibration bands and –N=N– vibration band were observed within the range 3349 – 3302 cm^{-1}, 2922 – 2883 cm^{-1}, and 1566 – 1469 cm^{-1} respectively. The shifts of the peaks of this vibration in the complexes ranging between 12 and 8 cm^{-1} depending on the ligands suggested complexation. The vibrational frequencies of the imine group were within the range 1653 – 1615 cm^{-1} and appeared at a different wavenumber than the –HC=N vibrational frequencies of the ligands [26]. New bands corresponding to M-N and/or M-O vibrations appeared in the IR spectra of the complexes. Both of the bands corresponding to these vibrations were observed only in the $[Pt(3,5\text{-Br-Sal-Tet})H_2O] \cdot ClH_2O$ complex. In the other complexes, only bands belonging to the M-N vibration could be observed.

The ^1H NMR spectra of the [Pt(5-Br-Sal-Tet)Cl] and $[Pt(3,5\text{-Br-Sal-Tet})] \cdot Cl$ complexes were carried out in DMSO-d_6. The ^1H spectra of the complexes are demonstrated in Figure 3A. A peak of the phenolic-OH group is observed as a singlet at 11.44 ppm [27, 28] owing to coordination or crystal water. The azomethine proton (CH=N) in the [Pt(5-Br-Sal-Tet)Cl] complex appears as a weak singlet at 8.98 ppm, whereas the azomethine proton of the $[Pt(3,5\text{-Br-Sal-Tet})] \cdot Cl$ appears as a singlet at 9.87 ppm. The aromatic ring protons are observed in the 7.48 – 6.89 ppm range as expected.

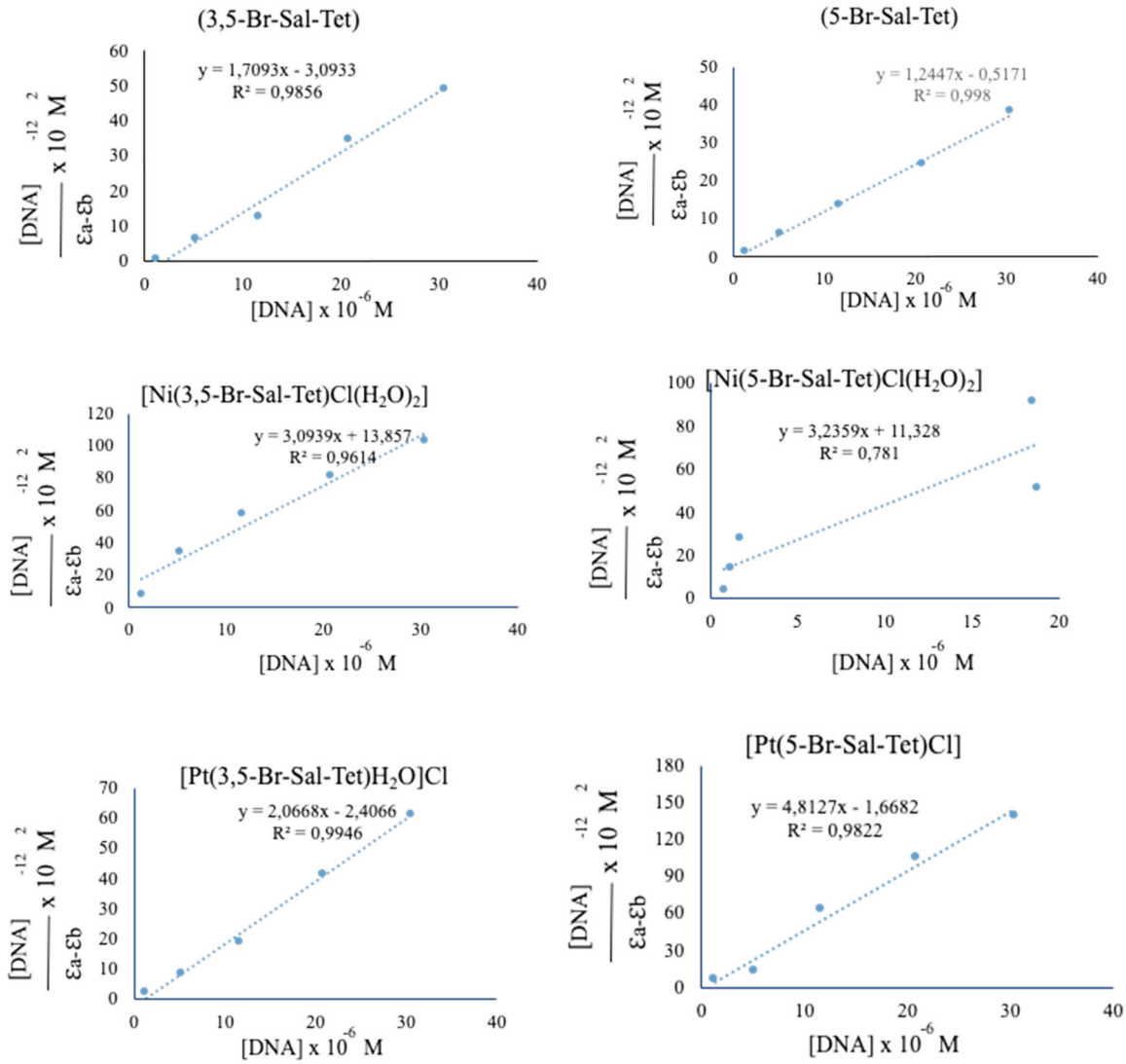

Fig. 6. [DNA]/ ε_a-ε_b, [DNA] plots for the determination of the binding constant of ligands–DNA and complexes–DNA.

TABLE 4. The Binding Constant (K_b) with DNA and Spectroscopic Investigation of Interaction with Tetrazolato-Schiff Bases and Their Ni(II) and Pt(II) Complexes

Compound	$K_b \times 10^4$ (L/mol)	DG° (kJ/mol)	%H
(5-Br-Sal-Tet)	21.5	-7.48	48.30
$[Ni(5\text{-Br-Sal-Tet})Cl(H_2O)_2] \cdot 2H_2O$	nsc	–	–
$[Pt(5\text{-Br-Sal-Tet})Cl] \cdot H_2O$	25.8	-7.94	50.30
(3,5-Br-Sal-Tet)	4.90	–3.89	86.81
$[Ni(3,5\text{-Br-Sal-Tet})Cl(H_2O)_2] \cdot 2H_2O$	1.99	–1.68	61.15
$[Pt(3,5\text{-Br-Sal-Tet})H_2O]Cl \cdot H_2O$	76.7	–10.61	22.59

nsc: no significant calculation was made in the standard operating condition.

The ^{13}C NMR spectrum of the $[Pt(3,5\text{-Br-Sal-Sal-Tet})H_2O]Cl \cdot H_2O$ complex was compared with the corresponding ligand. It was predicted that the chemical shift values of the aromatic carbon peaks might be within the range 140.00 – 111.70 ppm and the chemical shift value of the –CH=N– group might be at 152.00 ppm. The chemical shift value of the carbon atom connected to the –O group in the aromatic ring of the $[Pt(3,5\text{-Br-Sal-Tet})H_2O]Cl. H_2O$ complex was interpreted as 156.41 ppm.

3.2. DNA Studies

Viscometry Experiments for Tetrazolato-Schiff Bases and Their Complexes

An evaluation was made by comparing the similarities to the plot formed as a result of viscosimetric measurements of the interaction of the intercalating agent ethidium bromide with ct-DNA.

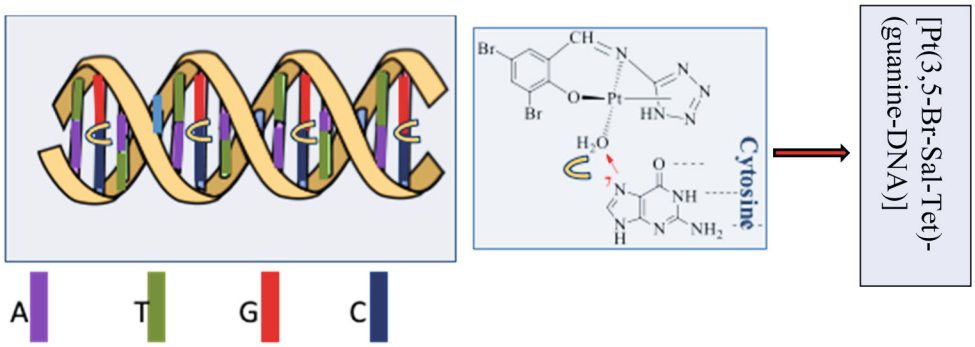

Fig. 7. Schematic illustration of the formation of [Pt(3,5-Br-Sal- Tet)-(guanine-DNA)].

Sources suggest that the interaction of ethidium bromide with ct-DNA might be an intercalation type. The $(\eta/\eta o)^{1/3}$ plot of [compound[/[DNA] against $(\eta/\eta o)^{1/3}$ for all Schiff bases and their complexes is similar to that of ethidium bromide (Fig. 4A). Therefore, it may be said that the interactions of these compounds with DNA are of the intercalation type. In fact, it is seen from the graphs that Pt(II) complexes give a better result.

G-quadruplexes are four-stranded structures found at the telomeres of DNA. Telomeres, located at the ends of linear chromosomes, are nucleoproteins associated with cell growth [27]. It is stated that cell death occurs when telomeres are reduced. When the G-quadruplex structure interacts with a small molecule, telomere elongation stops [30] and this can lead to cell death.

The square-planar geometry of the G-quadruplex DNA structure allows Pt(II) complexes to interact via intercalation [31].

The formation of a graph as in Figure 5, the interaction of Pt(II) complexes with DNA by intercalation may be due to both the square-planar structure and the small molecular size compared with Ni(II) complexes. It may be possible for these complexes to make an intermolecular P–P stacking mode with four-stranded structures in telomeres (Fig. 4B).

UV-Visible Spectroscopic Experiments for tetrazolato-Schiff bases and their complexes

To find the ct-DNA binding constant values (K_b) of the complexes, the [DNA]/(εa–εf) values versus the concentration values [DNA] were graphed. K_b was calculated using the slope of the line in the graph (Figs. 5, 6, and Table 4).

According to the electronic absorption spectra showing the interaction of ligands and complexes with ct-DNA (except [Ni(5-Br-Sal-Tet)Cl(H_2O)$_2$]), an increase in absorbance values and a blue shift in wavelength (2 – 5 nm) was observed by adding ct-DNA. This result suggests that the possible mode of interaction of all studied compounds with ct-DNA is electrostatic interaction or binding to DNA minor/major grooves. As seen in Fig. 6*a* hyperchromic effect was observed in all complexes. This effect is observed when DNA is denatured. Among the complexes, the graph of [Pt(3,5-Br-Sal-Tet)H_2O]Cl · H_2O was more significant. This may be due to the ionic nature of complex [Pt(3,5-Br-Sal-Tet)H_2O]Cl · H_2O.

The large K_b constant in the [Pt(3,5-Br-Sal-Tet)H_2O] complex indicates that the interaction with DNA is strong and the large DG^o indicates that this interaction is spontaneous. The reason for this is that the water molecule in the [Pt(3,5-Br-Sal-Tet)H_2O] complex is easily replaced by guanine, thus forming [Pt(3,5-Br-Sal-Tet)-(guanine-DNA)] [32] (Fig. 7).

3.3. Biological activity of tetrazolato Schiff bases and their complexes

Tetrazolato Schiff bases and their complexes were screened for antimicrobial activity in DMF solvent as a control substance. The compounds were tested with the same concentrations in DMF solution. The ligands and the complexes were tested for their antimicrobial activity by the well-diffusion method. All the synthesized compounds and antibiotics exhibited varying degrees of inhibitory effects on the growth of different tested strains (Table 5, Figs. 8). Furthermore, compounds were more effective in Gram-positive bacteria than in Gram-negative bacteria (Table 5, Fig. 8).The possible reason for this may be the presence of the outer impermeable membrane, the presence of the periplasmic space, thin peptidoglycan monolayer and cell wall composition in Gram-negative bacteria, so the activity is observed less or narrowly [33]. All the compounds were active against *B. cereus*, *E. aerogenes*, *P. putida*, *S. typhi*, *E. coli*, and *C. albicans.*

Synthesized tetrazolato Schiff bases and their complexes were inactive against *M. luteus* except [Pt(3,5-Br-Sal-Tet)H_2O]Cl · H_2O. As seen in Table 5, we can say that Pt(II) complexes showed a better effect than Ni(II) complexes. In fact, Pt(II) complexes showed an even better effect than their ligands. Only complex [Pt(3,5-Br-Sal-Tet)H_2O]Cl · H_2O showed activity against all the microorganisms studied.

Furthermore, the antibacterial activity of tetrazolato Schiff bases and their complexes was also compared with

four commercial antibiotics and antifungals, namely, kanamycin, sulfamethoxazole, ampicillin, amoxycillin, and nystatin. It was seen that the synthesized compounds were as effective as the antibiotics mentioned.

The effect of the [Pt(5-Br-Sal-Tet)Cl] complex against *P. putida* was as effective as all the drugs studied. As shown in Table 1, the [Ni(5-Br-Sal-Tet)Cl] complex was as effective as kanamycin (K30) against *S. epidermis*, the [Pt(5-Br-Sal-Tet)Cl] complex was as effective as sulfamethoxazole (SXT25) against *S. aureus*, and the complex [Pt(3,5-Br-Sal-Tet)H_2O]Cl was as effective as amoxycillin (AMC30) against *B. cereus*.

Kanamycin (K30), known to have side effects, is an antibiotic used in the treatment of serious bacterial infections and tuberculosis. It is an important result that the synthesized compounds [Ni(5-Br-Sal-Tet)Cl$(H_2O)_2$] and [Pt(3,5-Br-Sal-Tet)H_2O]Cl complexes show activity, although they are less antibacterial than K30. Tetrazolato-Schiff Bases and Ni(II) and Pt(II) complexes were more effective against *S. typhi* causing typhoid disease than the drugs SXT25, AMP10, and AMC30.

TABLE 5. Antimicrobial Activity of Tetrazolato-Schiff Bases and Ni(II) and Pt(II) Complexes (0.018 μg/ml) (diameter of zone of inhibition (mm))

		(5-Br-Sal-Tet) Ni(II) Pt(II)	(3, 5-Br-Sal-Tet) Ni(II) Pt(II)	*AMP10*	*SXT25*	*AMC30*	*K30*	*NYS 100*
	M. luteus	– – –	– – 10 ± 0.2	22 ± 0.1	21 ± 0.2	25 ± 0.1	23 ± 0.1	NT
Yeat Gram (-)	*S. epidermis*	23 ± 0.1 24 ± 0.1 22 ± 0.2	23 ± 0.3 – 10 ± 0.2	26 ± 0.1	25 ± 0.1	27 ± 0.3	25 ± 0.2	NT
	S. aureus	22 ± 0.3 18 ± 0.2 23 ± 0.1	22 ± 0.2 – 18 ± 0.3	30 ± 0.2	24 ± 0.1	30 ± 0.2	25 ± 0.2	NT
	B. cereus	13 ± 0.2 14 ± 0.1 16 ± 0.2	13 ± 0.2 13 ± 0.3 19 ± 0.1	23 ± 0.1	25 ± 0.2	20 ± 0.1	28 ± 0.1	NT
Gram (+)	*P. putida*	19 ± 0.3 19 ± 0.3 26 ± 0.1	16 ± 0.2 18 ± 0.2 19 ± 0.3	8 ± 0.1	18 ± 0.2	15 ± 0.2	14 ± 0.2	NT
	K. pneumoniae	– 12 ± 0.1 –	– – 12 ± 0.1	21 ± 0.3	20 ± 0.2	21 ± 0.1	23 ± 0.1	NT
	E. aerogenes	12 ± 0.2 12 ± 0.2 14 ± 0.3	13 ± 0.1 12 ± 0.2 15 ± 0.1	21 ± 0.2	19 ± 0.2	20 ± 0.2	24 ± 0.2	NT
	S. typhi	23 ± 0.1 20 ± 0.2 20 ± 0.2	22 ± 0.2 20 ± 0.3 24 ± 0.2	11 ± 0.3	17 ± 0.1	19 ± 0.2	20 ± 0.2	NT
	E. coli	20 ± 0.2 15 ± 0.1 19 ± 0.2	17 ± 0.3 15 ± 0.2 16 ± 0.2	10 ± 0.1	18 ± 0.2	14 ± 0.1	25 ± 0.2	NT
	P. vulgaris	14 ± 0.3 – 10 ± 0.2	13 ± 0.2 10 ± 0.3 10 ± 0.2	17 ± 0.2	19 ± 0.1	20 ± 0.2	21 ± 0.1	NT
	C. albicans	26 ± 0.2 30 ± 0.3 30 ± 0.2	14 ± 0.3 20 ± 0.2 23 ± 0.2	NT	NT	NT		20

* SXT25, sulfamethoxazole; AMP10, ampicillin ; K30, kanamycin; AMC30, amoxycillin; NYS, nystatin, NT, not tested; diameter of zone inhibition (mm)

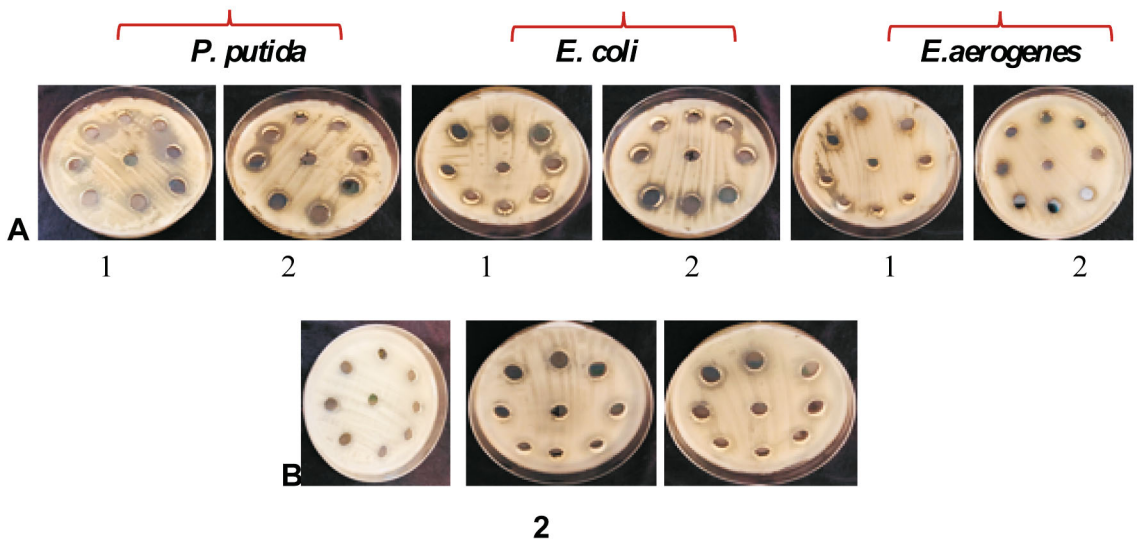

Fig. 8. **A:** Zone images of (Tet-SalH-F-CH_3-Pt) and (Tet-SalH-F-Cl-Pt) against some pathogenic bacteria and yeast {1: (Tet-SalH-F-CH_3-Pt), 2: (Tet-SalH-F-Cl-Pt)}. **B:** Zone images of (Tet-SalH-F-Cl-Pt) against *P. vulgaris*, *S. epidermis*, and *S. typhi.*

4. CONCLUSIONS

In the ^{1}H NMR spectra of Schiff bases, as the number of halogen groups increases, the electron density of the molecule becomes lower, so the peak of molecule (3,5-Br-Sal-Tet) appeared in the low field. When the FT-IR spectra of the complexes are compared with the spectra of the tetrazolato ligands, the appearance of the peaks belonging to the imine group in a different region is due to complexation.

The fact that the new tetrazolato compounds show very good antimicrobial activity at very low concentrations shows that we have achieved our aim. Tetrazolato Schiff bases and their complexes can certainly compete with and even outperform commercial antibiotics–antifungals used in the treatment of microbial infections. Therefore, it is believed that these resulting compounds can be used as excellent antimicrobial agents against pathogenic microorganisms or as an additive to antimicrobial products.

Ultraviolet-visible region spectroscopy experiments revealed that the type of interaction of the studied molecules with DNA is electrostatic or binding to minor/major grooves between base pairs of DNA and aromatic chromophore. Viscometry experiments suggested that all Schiff bases and complexes might also have intercalation-type interactions with DNA. It is rare for tetrazolato Schiff bases and complexes to show electrostatic, minor/major groove binding and intercalation-type interactions with DNA.

Acknowledgements

The authors would like to thank Gazi University Scientific Research Projects Coordination Unit.

Conflicts of interest statement

The authors declare that there are no conflicts of interest.

Author contributions

N. Sarı conceived and planned the experiments and contributed to the interpretation of the results. M. Ulular contributed to synthesis and characterization. F. Han studied the DNA binding effects of the substances and H. Öğütcü studied their antimicrobial effects. N. Sarı and E. Hasanoglu Özkan contributed significantly to the shaping of the article.

Funding statement

This study is funded by Scientific Research Projects Coordination Unit of Gazi University 05/2018-17.

REFERENCES

1. S. Sayed, S. Dawood, S. Ibrahim, et al., *Biointerface Res. Appl. Chem*., **10**(6), 6936 – 6963 (2020).
2. D. E. Reichert, J. S. Lewis, C. J. Anderson, *Coord. Chem. Rev.*, **184**(1), 3 – 66 (1999).
3. D. Nartop, P. Gürkan, N. Sarı, et al., *J. Coord. Chem*., **61**(21), 3516 – 3524 (2007).
4. N. Sarı, N. Pişkin, H. Öğütcü, et al., *Med. Chem. Res*., **22**(2), 580 – 587 (2013).
5. K. C. Emregül, E. Düzgün, O. Atakol, *Corros. Sci*., **48**(10), 3243 – 3260 (2006).
6. J. Zhang, S. Wang, Y. Ba, et al., *Eur. J. Med. Chem.*, **178**, 341 – 351 (2019).
7. Y. Yıldırır, M. F. Us, N. Çolak, et al., *Med. Chem. Res*., **18**(2), 91 – 97 (2009).
8. C.-X Wei, M. Bian and G.-H. Gong, *Molecules.*, **20**(4), 5528 – 5553 (2015).
9. G. I. Koldobskii, V. A. Ostrovskii and B. V. Gidaspov. *Chem. Heterocycl. Compd.*, **16**(7), 665 – 674 (1980).

10. S. Yavuz, O. Aydın, S. Çete, et al., *Med. Chem. Res.*, **19**(2), 120 – 126 (2010).
11. R. L. Siegel, K. D. Miller, A. Jemal, et al., *Ca: Cancer J. Clin.*, **66**(1), 7 – 30 (2016).
12. A. Di Lorenzo, M. T. Bedford, *FEBS Lett.*, **585**(13), 2024 – 2031 (2011).
13. A. R. Katritzky, C. A. Ramsden, E. F. V. Scriven, R. J. K. Taylor, *Comprehensive Heterocyclic Chemistry III*, Vol. 6: *Other Five-membered Rings with Three or more Heteroatoms, and their Fused Carbocyclic Derivatives* (2008), pp. 257 – 423.
14. Y. Tao, J. R. Li, Z. Chang, et al., *Cryst. Growth Des*., **10**(2), 564 – 574 (2010).
15. N. Fischer, T. M. Klapötke, S. Scheutzow, et al., *Cent. Eur. J. Energ. Mater.*, **5**(3 – 4), 3 – 18 (2008).
16. J. Vanco, Z. Sindelar, Z. Dvorak, et al., *J. Inorg. Biochem*., **142**, 92 – 100 (2015).
17. R. Bera, B. K. Sahoo, K. S. Ghosh, et al., *Int. J. Biol. Macromol*., **42**(1), 14 – 21 (2008).
18. S. Niloufar, D. S. Farzad, B. Sima, et al., *J. Biomol. Struct. Dyn.*, **37**(2), 359 – 371 (2019).
19. D. Nartop, B. Demirel, M. Güleç, et al., *J. Biochem. Mol. Toxicol*., **34**(2), e22432 (2019).
20. S. Koçoğlu, H. Öğütcü, Z. Hayvalı, Res. *Chem. Intermed*., **4**(45), 2403 – 2427 (2019).
21. S. Rubab, S. Bahadur, U. Hanif, et al., *Biocatal. Agric. Biotechnol.*, **31**, 101894 (2021).
22. I. Sakıyan, E. Logoglu, S. Arslan, et al., *Biometals*, **17**(2), 115 (2004).
23. A. A Popov, V. M. Senyavin, A. A. Granovsky, *Fuller. Nanotub. Carbon Nanostruct*., **12**(1 – 2), 305 – 310 (2005).
24. D. Sinirliogglu, A. E. Müftüoglu, A. Bozkurt, *J. Polym. Res.*, **20**, 242 – 250 (2013).
25. R. M. Silverstein, G. C. Bassler, T. C. Morrill, *Spectrometric identification of organic compounds*, 4. Edition Jhon Wiley and Sons Inc USA (1981).
26. G. C. Percy, D. A. Thornton, *J. Inorg. Nucl. Chem*., **34**(11), 3357 – 3367 (1972).
27. S. Yavuz, Y. Unal, O. Pamir, et al., *Arch. Pharm.*, **34**(6), 455 – 462 (2013).
28. Y. Yildirir, O. Pamir, S. Yavuz, et al., *J. Heterocycl. Chem*., **50**(S1), E93 – E99 (2013).
29. E. H. Blackburn, *Nature*, **408**, 53e56 (2000).
30. S. Artandi, S. L. Chang, S. Lee Alson, et al., *Nature*, **406**, 641 – 645 (2000).
31. Y. Sun, Y. Lu, M. Bian, et al., *Eur. J. Med. Chem*., **211**, 113098 – 113105 (2021).
32. T. C. Johnstone, K. Suntharalingam, S. J. Lippard, *Chem. Rev.*, **116**(5), 3436 – 3486 (2016).
33. J. Afzal, N. Ullah, Z. Hussain, et al., *Matrix Science Pharma*, **1**(2), 17 – 19 (2017).